Volume 11
Number 38
14 October 2023
Pages 20275–20856

Journal of Materials Chemistry A

Materials for energy and sustainability

rsc.li/materials-a

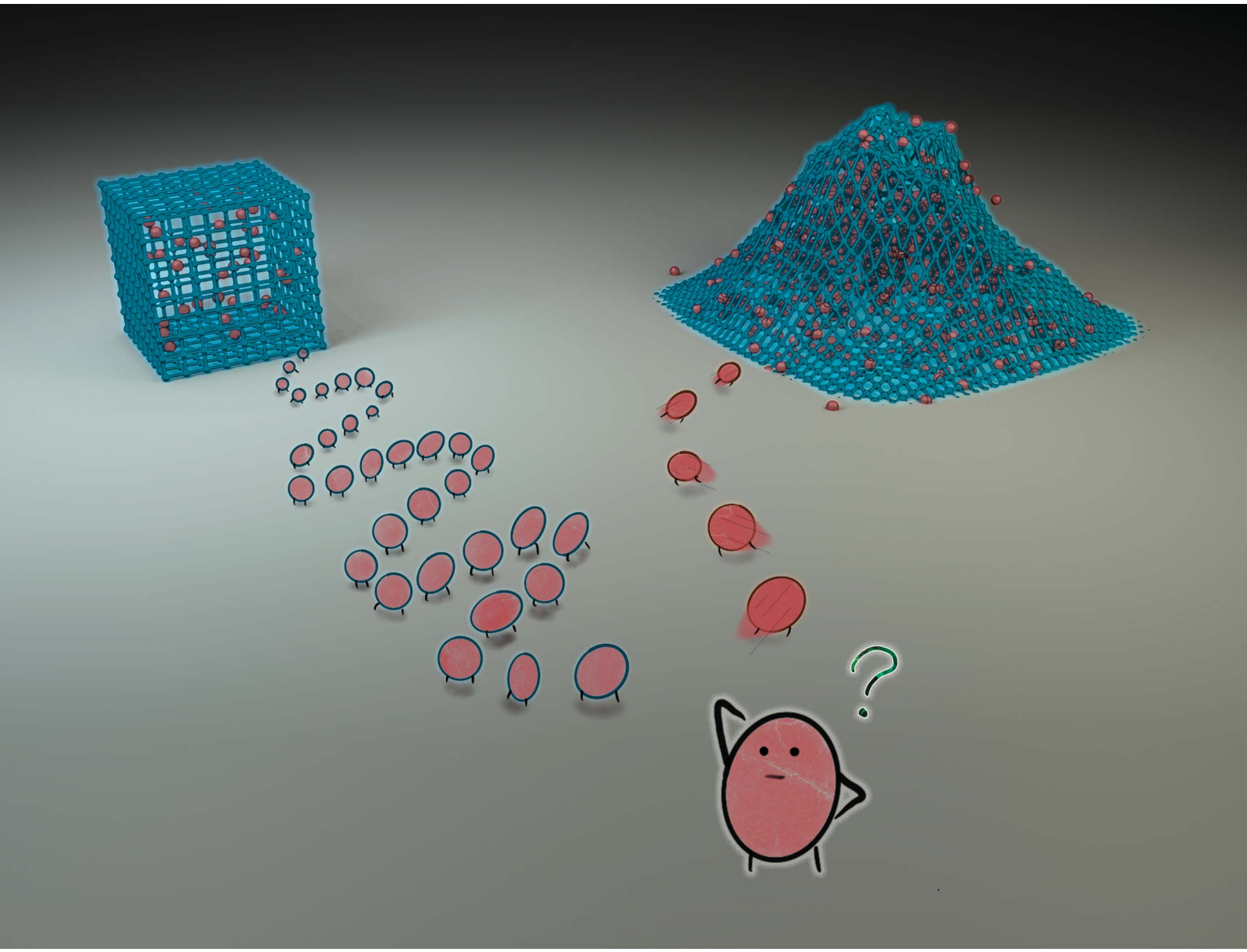

ISSN 2050-7488

ROYAL SOCIETY OF CHEMISTRY

PERSPECTIVE
Jingwei Hou *et al.*
Ion transport and conduction in metal–organic framework glasses

10 YEARS ANNIVERSARY

Journal of Materials Chemistry A

ROYAL SOCIETY OF CHEMISTRY

PERSPECTIVE

View Article Online
View Journal | View Issue

Cite this: J. Mater. Chem. A, 2023, 11, 20302

Ion transport and conduction in metal–organic framework glasses

Milton Chai,[a] Ruiqi Chen,[a] Kaijie Xu,[a] Yuelei Chen,[a] Shengchun Ma,[a] Rijia Lin,[a] Vicki Chen[b] and Jingwei Hou *[a]

Metal–organic frameworks (MOFs) are a group of highly tunable porous materials composed of metal nodes and organic linkers. Although MOF research has predominantly focused on crystalline frameworks, amorphous MOFs with disordered structures have seen a surge in interest over the past few years. In particular, an emerging subgroup of amorphous MOFs exhibiting a glass transition temperature, known as MOF glass, offers several benefits as an ion conductor including the absence of grain boundaries, isotropic properties and high moldability. This perspective aims to explore the recent developments in MOF glass materials for ion transport and conduction. The mechanism and underlying factors that govern ion transport properties will be elucidated to guide the design of these materials with enhanced ion conductivity and selectivity. We also highlight their latest applications for electrochemical and energy related systems. Finally, we offer prospective strategies for tuning the ion transport characteristics in MOF glass to direct its implementation in current and future applications.

Received 30th May 2023
Accepted 15th August 2023

DOI: 10.1039/d3ta03192f

rsc.li/materials-a

Introduction

Metal–organic frameworks (MOFs), also known as porous coordination polymers, are materials composed of metal nodes connected by organic linkers with potential voids in the architecture.[1] There are over 100 000 MOFs that have been experimentally characterised with a large variability in structure and composition, which enables them to be tailored for specific applications.[2,3] The majority of MOF research to date has focused on the crystalline domain, but there has been rising interest particularly over the past few years on the topic of structural disorder in MOFs. MOFs with an amorphous or disordered structure lack any long-range periodic order, but retain the basic building blocks and metal–ligand–metal connectivity of their crystalline counterpart, which usually leads to the retaining of the porosity, at least partially.[4]

Amorphous materials such as inorganic glasses are known to be excellent ion conductors since the early days of solid-state ionics.[5] Recent results of other porous materials such as covalent–organic frameworks (COFs), which are composed of organic components connected by covalent bonds, also indicate that decreased crystallinity can be favourable for ion conduction.[6,7] Nevertheless, regulating the crystallinity in COFs is more difficult than in MOFs due to the strong covalent bonds between organic building blocks compared to metal–ligand bonds in MOFs.[8] Over the past few years, a subgroup of amorphous MOF materials exhibiting a glass transition temperature, known as MOF glass, has emerged and rapidly gained research interest. It was discovered that certain MOFs, such as those from the zeolitic imidazolate framework (ZIF) family, undergo a solid to liquid phase transition below their decomposition temperatures and can subsequently form an amorphous glass upon cooling.[9,10] Since then, MOF glasses have been applied as ion conductors for batteries and fuel cells, where improvements in ion conductivity and selectivity are generally observed compared to their crystalline counterparts or other crystalline conductors.[11–14]

The general benefit of an amorphous MOF conductor with no long-range order is that it provides isotropic pathways for ion

[a]School of Chemical Engineering, University of Queensland, St Lucia, QLD 4072, Australia. E-mail: jingwei.hou@uq.edu.au
[b]University of Technology Sydney, 15 Broadway, Ultimo, NSW 2007, Australia

Dr Jingwei Hou received his PhD in chemical engineering from the University of New South Wales in 2015. He then joined the UNESCO Centre for Membrane Science and Technology (2015–2017) and the University of Cambridge (2017–2019) for his post-doctoral research. In 2019, he returned to Australia as an ARC DECRA Fellow at the School of Chemical Engineering, University of Queensland. In 2021, he was named the ARC Future Fellow. He is currently a senior lecturer and group leader of the Functional Materials Engineering (FME) Laboratory.

conduction. This leads to a homogeneous migration of ions, which suppresses the formation of dendrites and improves the cycling stability in batteries.[14,15] Additional benefits are offered by MOF glass, which include the formation of bulk material with no grain boundaries and high moldability.[16–18] The lack of grain boundaries is favourable for fast ion conduction as the activation energy for ions traversing across grain boundaries is usually significantly higher than the bulk material.[13,19] Moreover, the access to a liquid state enables MOF glass to be moulded into different shapes and films, facilitating their integration into devices such as batteries, fuel cells and sensors.[18,20]

Ion transport in MOF glass is generally a complex process, with several factors related to the pores, ligands and metal sites that can impact the ion transport properties. This perspective will provide a critical view of the recent developments in amorphous MOFs with a focus on MOF glass for ion transport applications, which is an important area driving the sustainable energy future. We will shed light on the important factors that need to be considered for these materials to obtain enhanced ion transport properties. Furthermore, we will provide prospective tuning strategies and future research opportunities for developing MOF glass in this area.

Construction of MOF glass

The main approach to obtain MOF glass is to introduce disorder in crystalline MOFs through physical (mechanical milling, pressure), thermal (melt-quenching) or chemical stimulus. Among the physical stimuli, mechanical shear stress induced by ball milling is a fast and efficient route to obtain disordered MOFs by utilising hard balls to collide, grind, and stir against the MOF (Fig. 1a).[21,22] The progressive destruction of metal–linker bonds leads to framework defects and ultimately structural amorphisation.[23] It is possible to transform MOF crystals into a glassy state through ball milling, but MOFs with short metal–linker bond lengths (<2.19 Å) appear to be restricted by this strategy.[11,24] The compression of MOFs by external pressure is another approach to produce glassy MOFs (Fig. 1b).[25] However, this method is not as easily accessible which sometimes requires pressures greater than 100 MPa for non-rigid MOFs.[25,26]

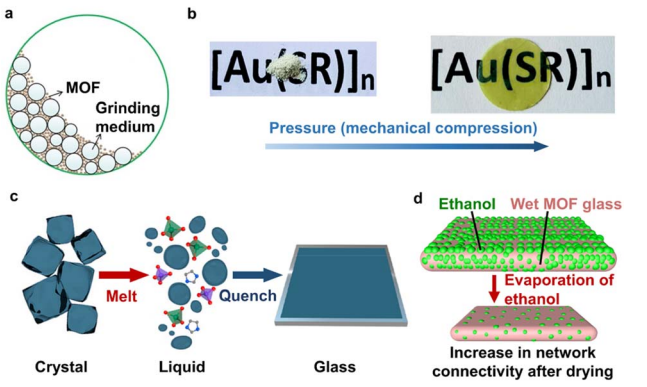

Fig. 1 (a) Amorphisation of MOF crystals into glass. Adapted with permission from ref. 22, copyright 2019 Elsevier B.V. (b) Compression by pressure of MOF powder into glass. Adapted with permission from ref. 25, copyright 2020 The Royal Society of Chemistry. (c) Melting of MOF crystals to the liquid phase followed by quenching to glass. Adapted with permission from ref. 27, copyright 2022 American Chemical Society. (d) MOF glass formed by evaporation of ethanol showed increasing connectivity with drying time. Adapted with permission from ref. 36, copyright 2023 Wiley-VCH GmbH.

Apart from the above-mentioned physical stimuli, MOF glass can also be formed through thermal treatment. The melt-quenching process is the most widely used strategy for transforming meltable MOFs into glass, which involves heating the MOF crystal to its melting point followed by rapid cooling (Fig. 1c).[9,27] Currently, meltable MOFs mainly stem from the ZIF family as well as metal-phosphate–azolate and metal–amide frameworks.[13,28–30] Further effort should be directed at lowering the melting temperature of MOFs to below their decomposition temperature to expand the types of meltable MOFs. This can be achieved by employing bridging ligands that form weak coordination bonds with metals (*e.g.,* sulfonates, esters, amides, and nitriles), which minimises the enthalpy change for the transition between solid and liquid phases.[30] On the other hand, maximising the entropy change through the utilisation of low-symmetry, high-flexibility ligands can also lower the melting point.[30] In addition, another strategy is to incorporate ionic liquids in the MOF structures to stabilise the dissociated linkers during heat treatment, which can also facilitate melting at a lower temperature.[31,32] It is expected that these strategies will be generally applicable to a wide range of MOFs, but their extension to MOFs with robust metal-linker bonds such as carboxylate-based MOFs remains limited so far.

In the efforts to further expand the construction of MOF glasses, several approaches that bypass the melting process have been recently developed involving the use of chemical stimuli or volatile solvent/modulator.[33–36] The selection of an appropriate chemical stimulus (*e.g.*, water vapour) to competitively coordinate to the metal nodes can form an amorphous framework that readily enters into a super-cooled liquid phase upon heating, which can then be vitrified.[33] Further research directed at the choice of chemical stimuli that can trigger the formation of this super-cooled liquid state in different frameworks is still required. In an alternate approach, a volatile solvent or modulator (*e.g.*, *m*-cresol and ethanol) with dissolved MOF precursors can be used, which acts to suppress MOF crystallisation during its gradual removal by evaporation (Fig. 1d).[34–36] This strategy has enabled the formation of a carboxylate-based MOF glass for the first time.[35] Given the infancy of these strategies, further understanding of the criteria and limitations on the wider applicability will be determined, but it is certainly promising.

Mechanism of ion conduction in MOF glass

Hitherto, most studies on MOF glass have centred on proton conduction as it is the most developed subgroup of ions. In the simplest case of proton conduction through MOF pores filled

with a conducting medium like H_2O, the protons can travel using either the Grotthuss mechanism or vehicle mechanism (Fig. 2). In the Grotthuss mechanism, protons hop along a chain of water molecules through concurrent hydrogen bond formation and cleavage, or alternatively along open metal sites in the MOF coordinated with OH^-/H_2O.[37,38] On the other hand, protons can also travel by attaching to a water molecule and migrating together as a hydronium ion.[39] Given that the energy requirement for hydrogen-bond cleavage is only 2–3 kcal mol^{-1} or 0.11 eV, site-to-site hopping of protons typically has a low activation energy of <0.4 eV.[40] In contrast, the diffusion of ionic carriers in the vehicle mechanism incurs larger energy penalty and thus usually has an activation energy of >0.4 eV.[40] This means that fast ion transport typically occurs *via* the Grotthuss mechanism. The migration of other ions such as Li^+ has also been explored in MOF glass containing ionic electrolytes and explained using similar mechanisms.[14]

In the absence of any water molecules, protons have been observed to be able to utilise the anionic sites in bridging ligands of MOF glass to hop along the framework (Fig. 2).[11,12] This enables the protons to migrate using a Grotthuss-like mechanism (site-to-site hopping) even under anhydrous conditions. Similarly, metal ions such as Li^+ can hop between the anionic sites of MOF linkers, or between the counter-ion sites coordinated to the metallic centres of MOF.[41,42]

In order to elucidate the ease of ion hopping between sites in solid ion conductors, the activation energy is often determined and compared. A larger activation energy typically denotes inhibition of ion hopping between neighbouring sites, or sometimes even a change in the conduction mechanism to the vehicle mechanism.[43] According to the Anderson–Stuart model for ion conduction in amorphous structures, the total activation energy is a summation of the electrostatic binding energy and strain energy.[44,45] The binding energy is the energy needed by the ion to overcome coulombic forces acting on it and leave its charge-compensating site.[46] Meanwhile, the strain energy is the energy required to move the ion from one site to another and is directly related to the jump distance.[47] The activation energy can be determined experimentally by fitting temperature-dependent conductivity to the Arrhenius equation:[11]

$$\sigma = (\sigma_0/T)\exp(-E_a/k_BT) \quad (1)$$

The terms σ, σ_0, T, E_a, and k_B denote the conductivity, pre-exponential factor, temperature, activation energy and Boltzmann constant respectively. Deviations from the Arrhenius behaviour may arise for glass-forming MOFs above the glass transition temperature (T_g), in which the Vogel–Tamman–Fulcher (VTF) equation would be more appropriate:[48]

$$\sigma = (\sigma_0/\sqrt{T})\exp(-E_a/k_B(T - T_0)) \quad (2)$$

T_0 represents the pseudo-glass transition temperature at which the ions become immobile, which is usually approximated to be 50 °C below T_g.[49] The behaviour described by the VTF equation is commonly found in viscoelastic systems such as glass and polymer conductors, and certain MOF glasses have also been observed to follow this relationship.[50]

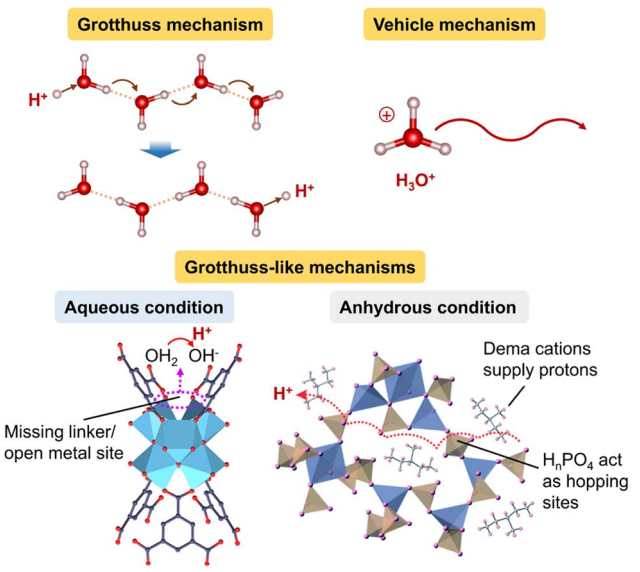

Fig. 2 Ion transport mechanisms exemplified by protons using Grotthuss, vehicle and Grotthuss-like mechanisms. Adapted with permission from ref. 12 (copyright 2020 The Royal Society of Chemistry), ref. 37 (copyright 2022 American Chemical Society) and ref. 38 (copyright 2019 Springer Nature).

Considerations for enhanced ion conductivity

Ion conductivity is a product of the charge of the ion, ion concentration and ion mobility (velocity under an electric field).[51] The latter two open pathways for further modifications in MOFs to enhance the ion conductivity. Defect engineering in crystalline MOF is known to be an effective strategy to increase both the ion concentration and mobility, enabling improvements in ion conductivity by 2–3 orders of magnitude compared to the low defect variant.[37,51] For example, Basu *et al.* prepared MOF-808 exhibiting super-protonic conductivity ($>10^{-1}$ S cm^{-1}) by inducing missing linker defects, which created Lewis acid open metal sites that were coordinated with OH^-/H_2O.[37] This not only increased the concentration of mobile H^+ in the framework, but also increased the H^+ mobility due to increased porosity consequential of missing linkers. Furthermore, the presence of open metal sites in Cu-azolate and Mg-carboxylate MOFs also served as binding sites for the anions of liquid electrolytes, leading to a high density of mobile cations (*e.g.*, Li^+) for conduction.[41,52]

Given the influence of defects on ion conduction, one might deduce that an amorphous structure with an abundance of under-coordinated metal–ligand species would be highly favourable.[53] Indeed, this was explored by Tang *et al.* by preparing low crystallinity/amorphous metal organogel materials (MOGs), which usually have similar building blocks to MOFs.[54] Significant improvements in ion conductivity were observed compared to their crystalline MOF counterpart, where the lack of grain boundaries was also recognised as

a contributing factor for the improvement.[54] However, some shortcomings of gel materials are their poor mechanical and thermal stability. Glass-forming MOFs with high mechanical and thermal stability such as metal-phosphate–azolates and certain MOFs from the zeolitic imidazolate framework family (*e.g.*, ZIF-4) may be preferred, which have also exhibited ion conductivities that are at least an order of magnitude higher for the amorphous state than the crystalline counterpart.[11,14]

Nevertheless, it is important to note that not all amorphised MOFs are necessarily good ion conductors. There are several key factors that need to be considered to yield a MOF glass with high ion conductivity, including porosity, ligand vacancies/functionalisation and inclusion of guest molecules.

Porosity

An important consideration for amorphised MOFs like MOF glass that still needs to be addressed is porosity as it can affect the ion mobility and is currently a subject of active research. Upon amorphisation of MOF crystals by heat, pressure or mechanical means, the accessible porosity is typically reduced due to the collapse of the porous framework.[23] Although protons have been observed to migrate effectively through an essentially nonporous framework, the same is not the case for other ions such as Li^+.[11,55] It is postulated that the formation of dead-end pathways from pore collapse impeded Li^+ migration, which led to some observations that amorphisation decreased the ion conductivity.[55] Therefore, exploring means to improve the porosity is favourable for ion conduction as it enhances the mobility of ions and provides more pathways for ion transport.

The measurement of porosity in MOFs is commonly done using a probe gas like CO_2 to determine the accessible surface area. It should be noted that MOF glasses from the ZIF family are found to be almost non-porous to N_2 (3.64 Å), and thus CO_2 (3.3 Å) with a smaller kinetic diameter is more appropriately used.[56] Alternatively, Positron Annihilation Lifetime Spectroscopy (PALS) can also be used to determine the porosity but may overestimate the pore sizes.[57] Henke and colleagues measured the CO_2 sorption at 195 K for ZIF glasses and determined the BET surface areas to be a_gZIF-4 (187 $m^2\ g^{-1}$) < a_gZIF-62 (200 $m^2\ g^{-1}$) < a_gTIF-4 (204 $m^2\ g^{-1}$).[58] Although these are an order of magnitude lower than the surface areas typically exhibited by crystalline MOFs, significant progress has been made over recent years to improve the porosity of MOF glasses.

Yaghi, Angell and colleagues presented a generalisable strategy of preparing high porosity MOF glass by using a plasticiser-modulator solvent (*m*-cresol) into which Ti metal nodes and bisphenol ligands are dissolved.[34] Evaporation of the volatile *m*-cresol solvent resulted in vitrification yielding a MOF glass that is porous to N_2, and has a surface area of 330 $m^2\ g^{-1}$ based on N_2 adsorption isotherms.[34] Their recent study further improved this strategy by using carboxylate linkers, along with *m*-cresol that acted as a modulator to competitively coordinate to the Ti-oxo cluster and is present in the framework.[35] The robust carboxylate linkages to the Ti-oxo cluster allowed for subsequent complete substitution of *m*-cresol with methanol without damaging the structural integrity, which yielded the highest porosity MOF glass by far with a N_2 BET surface area of 923 $m^2\ g^{-1}$ (Fig. 3).[35]

A more destructive strategy was also proposed by Feng *et al.* by immersing a_gZIF-76 in ammonia to induce missing-metal defects, which made it porous to N_2 with a surface area of 265 $m^2\ g^{-1}$.[59] Very recently, Yang *et al.* demonstrated that the incorporation of low molecular weight (M_w = 300) polyethyleneimine in ZIF-62 prior to melt-quenching can form glass with highly interconnected pores.[60] The formation of these pores in ZIF-62 glass was attributed to the evolution of gases (CO_2, NH_3 and H_2O) from the thermal decomposition of the added polymer.[60] It is envisioned that these fabrication methods may help to improve the ion conductivity in MOF glass.

Ligand vacancies/functionalisation

Protons and metal ions can utilise the anionic sites which are either coordinated to the metallic centres of MOF or on the MOF linkers to hop along the framework.[11,41] The density of the hopping sites is important to ensure that the ions have neighbouring sites to jump to. Furthermore, optimisation of the jump distance between sites and coulombic forces between ion and the site can also lower the activation energy for ion conduction.[44] Therefore, the ligand vacancies and ligand functionalisation of the MOF glass need to be carefully tuned for improved conductivity.

If the main conduction pathway is through ligand vacancies, it would be desirable to increase the density of these vacancies. This can be achieved through the utilisation of a coordination modulator (*e.g. m*-cresol) to competitively bind to the metallic centres during the construction of amorphous MOFs, which can later be substituted out with components like methanol that can provide ion hopping sites.[35,43] Alternatively, the use of thermolabile modulators like monocarboxylic acids can also form ligand vacancies after removal from heat treatment.[61] The density of hopping sites can then be tuned by adjusting the modulator concentration and controlling the degree of substitution/heat treatment.

On the other hand, the usage of functionalised linkers or anionic bridging ligands like $H_2PO_4^-$ in MOF glass can also provide sites for ion hopping.[13] Further modification of the functional moieties on the linkers is also possible through post-synthetic reactions.[62] Functional groups like sulfonate and carboxylate groups exhibit different binding energies to metal

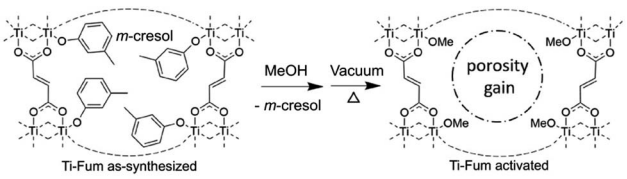

Fig. 3 Synthesis of high porosity Ti-fumarate MOF glass by utilising *m*-cresol as the coordination modulator, followed by complete substitution of *m*-cresol with methanol. Adapted with permission from ref. 35, copyright 2023 Wiley-VCH GmbH.

ions, which can be used to tune the activation energy for ion hopping.[63,64] For example, the binding energy of the sulfonate group to Li^+ is lower than that of the carboxylate group.[63,64] In order to adjust the jump distance between sites, a potential strategy that has yet to be explored is utilising a MOF such as ZIF-62 where the same metal nodes are coordinated with different types of linkers.[62,65] The activation energy can then potentially be tuned by adjusting the ratio of functionalised linkers.

Given that the main hopping pathway in this case is through the sites on the ligands, it would be favourable for the metal nodes to be fully coordinated. This was recently explored in a simulation work on a Zn-phosphate MOF glass, $(dema)_{0.35}[Zn(H_2PO_4)_{2.35}(H_3PO_4)_{0.65}]$, which showed that the conductivity can be increased up to 20 fold by increasing the Zn coordination number from 4.6 to 6.[66] This is because maximising the Zn coordination increases the density of ion hopping sites on the ligands, which increases the H^+ conductivity.[66] Nevertheless, the construction of this optimised structure has yet to be demonstrated experimentally. On a separate note, an interesting observation that has been made for this MOF glass is that varying the average microdomain size of its continuous networks changed the bulk phase viscosity, but did not significantly change the ion conductivity (Fig. 4).[67] This could be because the Zn coordination numbers were almost identical despite having different average microdomain sizes of continuous networks, which reinforces the notion that the coordination number of metal sites is the dominant factor regulating conductivity.[67] This also implies that not all of the coordinated ligands have to be bridged between two metal nodes, as long as the coordination number for each metal node is maximised for enhanced conductivity.

Incorporation of guest molecules

In the case where the activation energy barrier in MOF glass is still too high for Grotthuss-like conduction, one of the most common strategies to make it ionically conductive is to incorporate ionic liquids in the porous MOF structures as the guest molecules.[21,31] The transport of ions will be dominated by the diffusion of ionic liquid carriers in this case.[12] The benefit of structural amorphisation over retaining the crystalline MOF is that it can decelerate the exudation of guest molecules from the pores and hinder interactions between the guest molecules with ambient contaminants, which results in improved stability in ion conduction performance.[21,68]

In an ionically conductive MOF glass, the addition of dopants can further enhance the conductivity by supplying a high concentration of mobile ions for conduction. Acid molecules are often used to increase the concentration of mobile protons, while metal salts are commonly used to increase the concentration of mobile metal ions.[14,69] Dopants can be added directly during the amorphisation process prior to vitrification (*e.g.* melt-quenching, ball milling).[24,69] However, the requirement is that the dopant is able to withstand decomposition/degradation from the amorphisation process.

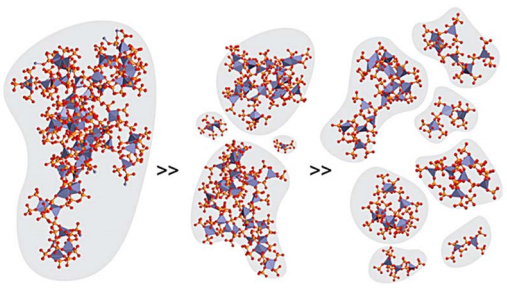

Fig. 4 $Zn–H_nPO_4$ frameworks showed little change in ion conductivity with a change in the connectivity of the coordination networks. The gray areas provide visual aids to distinguish the increasingly disconnected coordination network. Adapted with permission from ref. 67, copyright 2022 American Chemical Society.

Considerations for enhanced ion selectivity

Apart from conductivity, ion selectivity is another important characteristic for ion conductors especially for redox flow batteries, metal–sulfur batteries and ion separation/recovery applications.[70,71] Ion selectivity here refers to both charge selectivity such as between cations and anions, and also selectivity between similarly charged ions of different sizes and valency. The factors that should be considered for improving ion selectivity include the use of charged/functionalised linkers and pore morphology.

Charged/functionalised linkers

The functional groups on MOF ligands can be used to tune the charge selectivity. Charged functional groups that are protonated (positively charged) or deprotonated (negatively charged) can attract counter ions to the surface of MOF pores and form an electrical double layer (EDL). The EDL consists of a layer of counter ions immobilised on the pore surface (Stern layer) and a diffuse layer, which is characterised by the Debye length ($\lambda_D = 0.304/\sqrt{\text{ionic strength at 25 °C}}$).[72,73] If the MOF pore size is small enough such that the EDL overlaps, the counter ions become the dominant charge carrier in the pore channels. This results in a cation or anion-selective MOF, and can be characterised by the transference/transport number which is the ratio of the electric current derived from the target ion to the total electric current.[12,74]

Furthermore, the functional groups can also be tuned to achieve selectivity between ions of the same charge. Considerable effort has been placed over the past decade to develop ion-selective MOFs for the recovery of target ions such as Li^+ from other alkali and alkaline earth metal ions, but this has yet to be explored for MOF glass.[71,75,76] Functional groups like the sulfonate group have been used to effectively control the order of ion migration through MOF nanopores, which was attributed to the different binding affinities of ions like Li^+, Na^+ and K^+ to the sulfonate group.[64] Eisenman generalised the order of ion migration for hydrated alkali metal ions passing through

a functionalised/charged pore into a limited number of selectivity sequences, which is remarkably accurate despite its simplicity.[77] The key factor was attributed to the anionic field strength of the binding sites, which is a result of the competing phenomena between the attraction of ion to the charged binding site and the dehydration penalty for entering the site.[78]

Pore morphology

It is known that pore morphology can play a role in the separation of similarly charged hydrated ions. A MOF with one-dimensional pore channels like MIL-53 has little effect on the original transport rate of alkali metal ions in a bulk solution, and thus closely follows the ion migration order of $K^+ > Na^+ > Li^+$ in the bulk.[75] In contrast, the transport kinetics changes when the ions pass through a pore structure like UiO-66 comprised of different window (6 Å) and cavity (9–12 Å) sizes, where the ions need to undergo multiple dehydration and rehydration processes. The migration order becomes $Li^+ > Na^+ > K^+$, seemingly following the dehydrated ionic diameters as opposed to the hydrated diameters in bulk solution, which provides better ion sieving properties for the lithium recovery process.[75,76]

Bennett's group probed the pore size distribution of ZIF-4 glass using PALS, which revealed the presence of two different pore cavities with sizes of 2.6 Å and 6.9 Å.[57] Given that the limiting pore size is larger than the ionic diameter of Li^+ (1.20 Å), it is likely that Li^+ can migrate through ZIF-4 glass.[79] Indeed, ZIF-4 glass has been applied as a quasi-solid state electrolyte for lithium-ion batteries.[14] It is expected that alkali metal ions can also potentially undergo dehydration and rehydration processes in ZIF-4 glass for improved ion sieving properties, which bears further investigation.

Applications of ionically conductive MOF glass

Proton conduction

MOF glass can be applied as a solid-state proton conductor for batteries and fuel cells. In 2016, Kitagawa and Horike's group reported a Cd-phosphate–azolate MOF glass for the first time showing high anhydrous proton conductivity and dielectric constant that were two orders of magnitude higher than the crystalline counterpart.[11] A similar type of MOF glass with Zn nodes was later implemented in the demonstration of a rechargeable all solid-state anhydrous proton battery with a wide operating temperature range of 25–110 °C.[13] The high moldability of the MOF glass provided a flawless and grain-boundary free interface between the electrode and electrolyte, enabling proton migration at low activation energy (Fig. 5a and b).[13] In contrast, it was found that the charging and discharging processes were not even possible at 25 °C using the crystalline form of Zn-phosphate–azolate MOF.[13]

Although improvements in conductivity are often prioritised in the development of proton conductors for battery applications, the selectivity of protons is also important for applications such as fuel cells.[67] For example, a H_2/O_2 fuel cell utilising a solid glassy MOF electrolyte was observed to have a higher open-circuit voltage of 0.96 V compared to 0.88 V for a protic ionic liquid, which was attributed to the high proton transference number of the MOF (0.94) compared to the ionic liquid (0.49).[12] Given that there is typically a trade-off between conductivity and selectivity, a compromise in properties may be needed for the specific application of interest.[12,13]

An intriguing research study on certain proton-conductive MOFs like $Mg(HCO_2)_2$ and $Co(HCO_2)_2$ is the investigation of their ability to regulate (switch on and off) the conductivity, which may have applications in chemical sensors and biomimetic devices.[43,80] $Mg(HCO_2)_2$ and $Co(HCO_2)_2$ can exhibit no conductivity and high conductivity in the absence and presence of coordinated water molecules (2 per metal node) respectively, and this transformation between dehydrated and hydrated forms is reversible.[80] Similarly, a Zn-phosphate MOF glass with the ability to uptake water also showed conductivities differing by an order of magnitude under low (25%) and high (98%) relative humidity conditions (Fig. 5c).[43] It is likely that the density of supplied mobile protons and/or hopping sites governed this switch in conductivity.

Metal ion conduction

The conduction of metal cations including Li^+, Na^+ and Zn^{2+} have been investigated in amorphous MOFs including the MOF glass subgroup due to their promising applications as solid-state electrolytes, anode material and separator in batteries. A quasi-solid-state electrolyte composed of a ZIF-4 glass/lithium salt/polymer composite was utilised in a lithium-metal battery, which exhibited a higher Li^+ conductivity (0.161 mS cm^{-1} at 30 °C) than the polycrystalline counterpart (0.0821 mS cm^{-1}) due to the absence of grain boundaries.[14]

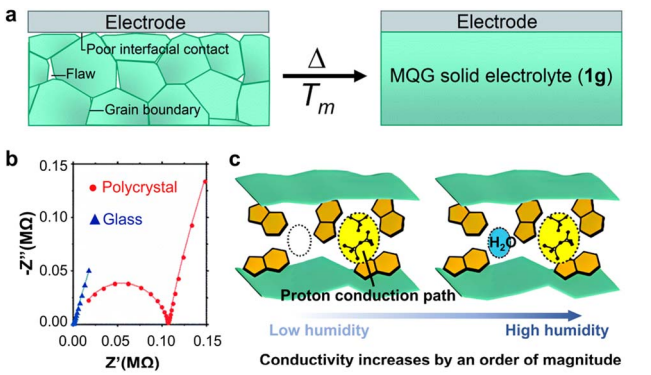

Fig. 5 (a) Melt-quenching of polycrystalline Zn-phosphate–azolate electrolyte into glass eliminated flaws at the electrode–electrolyte interface. (b) The melt-quenched MOF glass electrolyte showed only the bulk impedance response, while the polycrystalline MOF electrolyte showed additional response corresponding to the electrode–electrolyte interface. Adapted with permission from ref. 13, copyright 2021 The Royal Society of Chemistry. (c) Zn-phosphate MOF glass with water uptake ability showed increase in conductivity by an order of magnitude between low and high relative humidity conditions. Adapted with permission from ref. 43, copyright 2019 The Royal Society of Chemistry.

Furthermore, the cycling stability also improved significantly using ZIF-4 glass due to the suppression of dendrite formation.[14] This can be attributed to the lack of structural ordering in ZIF-4 glass, which provided statistically uniform ion flow in all spatial directions in the long range.[14] The voltage–time curve remained stable throughout 400 h of the long term cycling test conducted at 0.1 mA cm^{-2}.[14] In contrast, the ion flow in the ordered pores of polycrystalline ZIF-4 was anisotropic, leading to dendrite formation and cell failure after 217 h as indicated by a short circuit.[14] Interestingly, it is also possible to suppress dendrite propagation in other solid-state electrolytes like NASICON by melting a uniform layer of ZIF-62 on the electrolyte.[81] The layer provided uniform active sites that homogenised the interfacial Na^+/e^- flux in a Na-metal battery, which led to spatially even Na deposition.[81]

An important consideration on the use of MOF glass in the electrolyte component is electrochemical stability. A ZIF-4 glass composite was shown to have a stable electrochemical window of 2.3–4.0 V in a lithium-metal battery, which is adequate.[14] However, it would not be feasible to couple it with high-voltage cathodes like NCM-622 in the development of high-energy lithium batteries.[82] It should be noted that the polycrystalline counterpart had a higher oxidative stability to potentials of up to 4.7 V Li/Li^+, and thus it would appear that amorphisation can reduce the electrochemical window.[14] Given that MOF glass is still in the early stages of being implemented for battery applications, further research should be directed on this topic.

Apart from solid-state electrolytes, MOF glass can also be utilised as the anode material in batteries. A rather unexpected outcome has been observed when Co-ZIF-62 glass was used as the anode in Li-ion batteries.[83] Lithium insertion/extraction during the charge/discharge cycling process was found to disrupt the weak Co–N coordination bonds in MOF, which formed additional channels for Li^+ diffusion and storage (Fig. 6a).[83] The result is a continuous increase in Li-ion storage capacity up to triple of its initial value of 95 mA h g^{-1}.[83] A similar observation was also made for a Ni–ferrocene MOF.[84] The capacity can be further increased to 650 mA h g^{-1} through the encapsulation of Si nanoparticles, which by itself has a high theoretical specific capacity of >4000 mA h g^{-1}.[85] However, the large volumetric expansion (>300%) of pure Si during lithiation usually leads to its pulverisation.[86] Encapsulation of these nanoparticles in Co-ZIF-62 glass can buffer the volume changes and also prevent their aggregation for improved capacity retention during cycling (Fig. 6b).[85]

During the initial operation of a metal-ion battery, an electronically insulating but ionically conducting layer can form on the anode surface, which is aptly named the solid electrolyte interphase (SEI).[87] The formation of this layer consumes active metal ions and electrolyte materials leading to irreversible capacity loss, but at the same time it can also prevent further electrolyte decomposition once fully formed to ensure electrochemical stability.[88] Given that this layer is essentially a solid electrolyte, there is an opportunity to utilise MOF as an artificial SEI layer. This has been demonstrated for a structurally disordered Zr-based MOF, which is similar to MOF glass but does not exhibit a glass transition behaviour. The Zr-based MOF was applied as a coating to protect the Zn anode of a Zn-ion battery.[15] The artificial SEI layer offered several benefits that ultimately led to a long cycling life of 1800 h for the battery at a current density of 1 mA cm^{-2}, which include: (1) dangling bonds ($-PO_3H^-$ or $-PO_3^{2-}$) that provided Zn^{2+} hopping sites for migration and electrostatic shielding of anions in the electrolyte to inhibit side reactions, (2) pores that sieve pure Zn^{2+} for deposition and (3) isotropic conduction pathways that lead to smooth dendrite-free Zn deposition.[15] It is speculated that the implementation of MOF glass through melt-quenching may further eliminate any potential discontinuities in the artificial SEI layer.

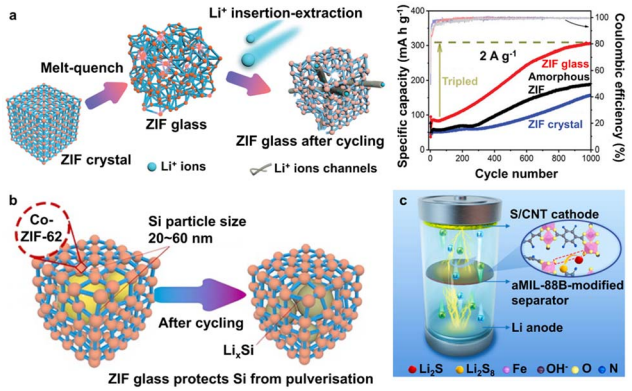

Fig. 6 (a) Capacity enhancement in the ZIF glass anode after cycling due to the formation of additional channels. Adapted with permission from ref. 83, copyright 2022 Wiley-VCH GmbH. (b) The ZIF glass anode protects encapsulated Si nanoparticles by buffering the volume changes and prolongs the cycling life. Adapted with permission from ref. 85, copyright 2022 Elsevier Ltd. (c) aMIL-88B separator inhibits polysulfide shuttling and improves the electrochemical performance. Adapted with permission from ref. 91, copyright 2021 Elsevier Ltd.

Aside from the conventional lithium-ion batteries (LIBs), a promising candidate for the next-generation of rechargeable batteries is lithium–sulfur batteries. This is due to the high theoretical specific capacity of the sulfur cathode of 1675 mA h g^{-1} (~10 times higher than that of conventional cathode materials in LIBs) and low cost.[89] However, a major shortcoming of this battery is the shuttle effect, in which soluble polysulfides generated from sulfur reduction at the cathode can migrate and react with the lithium anode to form inactive Li_2S.[90] Therefore, a separator allowing rapid Li^+ transport while inhibiting polysulfide shuttling is needed, which can be offered by amorphous MOFs like MOF glass. When crystalline MIL-88b was applied as a separator in a Li–S battery, it was observed that it could not inhibit polysulfide shutting effectively resulting in a low capacity retention of 382 mA h g^{-1} after 500 cycles at 1C.[91] In contrast, amorphised MIL-88b can effectively adsorb polysulfides and catalyse the polysulfide conversion kinetics due to higher exposure of active sites, resulting in increased capacity retention to 740 mA h g^{-1} (Fig. 6c).[91] Therefore, there is a promising opportunity for MOF glass to be applied as a separator.

Prospective tuning strategies for MOF glass and future applications

This section will focus on the prospective tuning strategies for MOF glass, which can be explored in future studies (Fig. 7). The high moldability of MOF glass potentially enables the construction of unique structures with enhanced ion transport kinetics. Furthermore, the accessibility of meltable MOFs to a liquid state prior to vitrification also offers opportunities for engineering of the ion transport at an interface. It is envisioned that these tuning strategies can extend the applications of MOF glass for ion sieving, pumping and sensing.

Heterogeneous MOF glass for unidirectional ion transport

A prospective strategy to impart unidirectional ion transport behaviour is to design a heterogeneous MOF glass with a pore size gradient. It is known that a nanopore with asymmetrical pore size and surface charge density can provide unidirectional ion transport, which is also referred to as ion rectification.[76] This behaviour is more commonly observed in asymmetrical polymer nanopores, but has also been observed recently in crystalline MOF-on-MOFs.[71,92] Unidirectional ion transport arises due to an ion concentration gradient induced by the asymmetrical distribution of surface charged groups along the pore, which enhances ion conduction in one direction but restricts conduction in the opposite direction.[76] The conduction of ion is typically favoured going from the narrow/tip side with high surface charge density to the larger/base side.[76] However, the favoured direction can be the reverse for the case of protons migrating *via* hopping between water molecules. Protons will preferentially travel from disordered to ordered water clusters as the energy barrier is nearly doubled in the other direction.[93] Ordered water chains are usually observed in sub-nanometre confinement, while the disordered form is more likely in a larger cavity (nanometre or above), and thus the preferred direction in this case is from the base-to-tip direction.[93]

The construction of a heterogeneous MOF glass can potentially be achieved by building up layers of different MOF glass through film casting and melt-quenching, which has yet to be explored. The requirement is that the highest melting temperature needs to be lower than the lowest decomposition temperature of the MOF glasses. The transition of MOF glasses to the liquid/molten phase upon heat treatment ensures good chemical reactivity at the interface.[53,94] This bypasses the issue of lattice mismatch as seen in crystalline MOFs, which provides a more versatile method for constructing MOF heterostructures.[95]

There are generally two strategies to prepare these multicomponent MOF glasses. The first is by heating different meltable MOFs above their melting temperatures, followed by vitrification which results in a blend with interlocking MOF domains.[96] The other utilises a meltable MOF to serve as a high temperature solvent for a secondary MOF component with no accessible melting point, which is referred to as flux melting.[97] There is a difference in the resulting interface between MOF domains for multicomponent MOF glasses prepared using these two strategies. Glass blends, such as the $(ZIF\text{-}4)_{0.5}(ZIF\text{-}62)_{0.5}$ blend, have been observed to have sharp interface regions with minimal diffusion between MOF phases due to the high viscosity of the liquid ZIFs.[98] On the other hand, flux melted MOF glasses such as $(ZIF\text{-}67)_{0.2}(ZIF\text{-}62)_{0.8}$ have a diffused interface region.[99] It is believed that liquid ZIF-62 initially penetrated into the structure of ZIF-67, and the flux-melting of ZIF-67 into a liquid state led to its diffusion back out of the ZIF-62 liquid.[99] This resulted in a larger inter-diffused region.

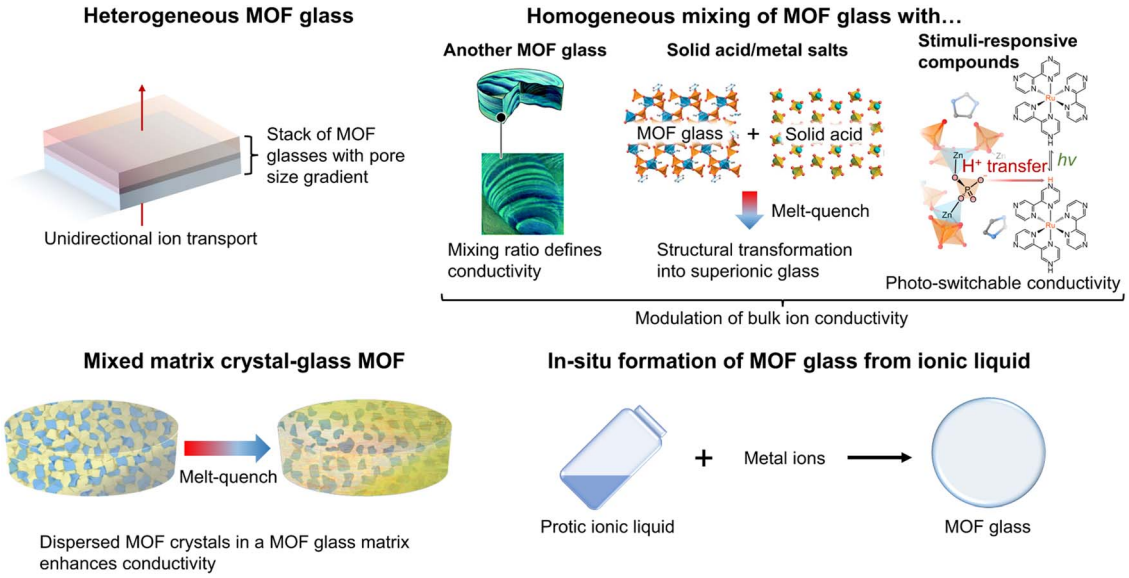

Fig. 7 Prospective tuning strategies for MOF glass including the construction of heterogeneous MOF glass, homogeneously mixed MOF glass, mixed matrix crystal–glass MOF and *in situ* formation of MOF glass from ionic liquid. Adapted with permission from ref. 12 (copyright 2020 The Royal Society of Chemistry), ref. 50 (copyright 2022 American Chemical Society), ref. 103 (copyright 2019 The Royal Society of Chemistry) and ref. 105 (copyright 2023 American Chemical Society).

The effect of these interfaces on ion transport in heterogeneous MOF glasses has yet to be determined. Nevertheless, observations from heterogeneous organic/organic, inorganic/inorganic and organic/inorganic interfaces may provide some insights.[100–102] Generally, heterostructures with a sharp transition region between layers of different pore sizes tend to suffer from low ion transport efficiency due to pore alignment mismatch and insufficient coupling between the different pore dimensions.[100] Therefore, interfacial engineering such as the use of a hydrogel interface is important to enhance interfacial ion transport.[100] It is also speculated that the conductance of ions across heterogeneous MOF glass with a diffused interface is higher than that with a sharp interface, due to better coupling of the pore dimensions between layers.

Homogeneously mixed MOF glass for modulation of bulk ion conductivity

The access of MOF glass to a liquid state enables a unique strategy for modulating the bulk ion transport properties. Two ionically conductive glass-forming MOFs with overlapping melting temperatures can be homogenised through mechanical mixing and subsequently melt-quenched.[16,103] Variation of the fraction ratios of the two MOF components would then allow for precise control of the bulk ion conductivity in mixed glass.[16] If the two MOF components have distinct glass transition temperatures in their pure forms, the formation of a homogeneous phase in the mixed glass can be verified through the observation of a single glass transition point, rather than two distinct points, which is indicative of a heterogeneous mixture.[16]

It is expected that this strategy can be further extended to modulate the conductivity of other homogeneous MOF glass mixtures such as with solid acids. It is known that solid acid compounds in the category of $MHXO_4$ and $M_3H(XO_4)_2$ [M = Cs, NH_4, Rb; X = S, Se] typically exhibit very low conductivities below their phase transition temperatures.[104] The interaction between a homogeneous mixture of MOF glass and solid acid during heat treatment can potentially lead to structural transformations forming a superionic mixed glass. For example, the exchange of oxyanions (HSO_4^- and phosphate) between $CsHSO_4$ solid acid and Zn-phosphate–azolate MOF during melt-quenching has been observed to yield structural changes with enhanced ion dynamics.[50] Interestingly, the conductivity of the mixed glass did not reside between that of the parent components, but rather at least an order of magnitude higher.[50] The modulation of ion transport properties through structural transformations in a mixed MOF glass system is relatively new, and opportunities still exist to explore other compounds such as metal salts (*e.g.* LiTFSI, $NaClO_4$).

Furthermore, the incorporation of stimuli-responsive compounds in mixed glass can also potentially modulate the bulk conductivity. Photo-responsive compounds such as pyranine and Ru-complex have been demonstrated to provide optically switchable proton conductivity in MOF glass, which is a promising start.[69,105] Other popular photo-responsive compounds such as azobenzenes and porphyrins can also be explored for a wider range of ions in future studies.[106,107] In addition, further possibilities exist to apply a photomask to achieve spatial control of the regions with low/high conductivities, which is worth exploring. Moreover, varying the concentration of the stimuli-responsive guest molecules in a hierarchical stack of MOF glass may also induce an ionic concentration gradient for unidirectional transport, which bears further investigation.

Mixed matrix crystal–glass MOF composites for enhanced ion conductivity

As discussed previously, amorphisation of crystalline MOFs does not always lead to improved ion conductivity as it depends on several factors such as porosity and optimisation of the hopping sites. In this case, the crystalline form with highly ordered pathways for ion conduction may have a higher ion conductivity through the bulk material.[55] However, a polycrystalline conductor with high intrinsic ion conductivity is often limited by large intergrain boundary resistance.[19] The term intrinsic here refers to ion conduction in the pores within the grain, as opposed to extrinsic conduction where ion travels along the interstices or interparticle phases. This emphasis is important as a significant portion of crystalline MOFs tested in the literature are in the polycrystal form (pellets) rather than single crystals, and discrepancies may arise due to the difficulty in determining whether conduction occurs intrinsically or extrinsically from impedance spectroscopy measurements.[108,109]

The intergrain boundary resistance for MOF polycrystals can be minimised by dispersing them in an ionically conductive MOF glass matrix. The high chemical reactivity of glass-forming MOF components in the liquid state during heating can provide good interfacial bonding and contact with the MOF crystals.[53,94,110,111] Compositing with MOF glass can potentially enhance the ion conductivity of crystal MOFs known to exhibit intrinsic conductivity such as lanthanide MOFs (PCMOF-5 family), which can be explored in future studies.[109]

In situ formation of MOF glass from ionic liquids

The incorporation of ionic liquids into MOF pores is a popular strategy to improve conductivity. However, it is important to note that both the cation and anion of ionic liquids are highly mobile, and hence the highest transport number for the ion of interest is typically still close to 0.5.[112] A unique strategy to improve the ion transport number, in this case of protons, was proposed by Horike's group by constructing a MOF glass *in situ* from a protic ionic liquid.[12] The reaction of Zn^{2+} with (dema)(H_2PO_4) ionic liquid formed an amorphous Zn^{2+}–$H_2PO_4^-$/H_3PO_4 network with entrapped dema cations.[12] Although suppressing the motion of both dema cations and H_2PO_4 anions of the ionic liquid might seem counterintuitive, the protons in the dema cations are mobile and can hop along the $H_2PO_4^-$ sites. This resulted in a high proton transport number of 0.94 compared to typical values of 0.5–0.6 for protic ionic liquids.[12] Interestingly, the proton conductivity of this MOF glass (13.3 mS cm^{-1} at 120 °C) was also double that of the protic ionic liquid (6.5 mS cm^{-1}).[12] This is reasonable as the

transport is now dominated by the Grotthuss mechanism, which typically has lower activation energy than the vehicle mechanism.[40] This proton conductivity is among the highest reported for MOFs and COFs.[113,114] It is envisioned that this strategy can potentially be extended to metal-salt-containing ionic liquids, *e.g.*, $[EMIM_{0.8}Li_{0.2}^{+}][TFSI^{-}]$, by the *in situ* formation of an amorphous MOF network with entrapped metal salts.[115] Alternatively, the anion of a metal salt could be covalently tethered to the organic ligand in a strategy analogous to that of single ion conductors for polymer electrolytes.[116,117]

Prospective applications

The high moldability of MOF glass due to the accessible transition between solid and liquid states allows for its facile integration into different device configurations. Various shapes can be achieved with MOF glass, which can be cast or pressed into films on substrates, sandwiched between electrodes and even pulled into fibers.[13,17,18] Although it has the potential to be implemented in a wide range of systems, the main application for an ionically conductive MOF glass currently is as a solid-state electrolyte for metal-ion batteries and fuel cells.[12–14] With further tuning of MOF glass, it is expected that the applications can be extended for ion sieving, ion pumping and ion sensing.

Tuning of the pore size, ligand functionalisation and density of hopping sites in MOF glass would allow for the sieving and recovery of critical mineral ions such as Li^{+}, Ni^{2+} and Co^{2+} from brines or spent batteries. The MOF glass can be cast as an ion-selective film/coating on a supporting substrate such as membranes or electrodes, or even hot-pressed into a free-standing MOF glass sheet. This can then be implemented in an electrodialysis or capacitive deionisation system for mineral recovery.[118,119]

Furthermore, the fabrication of heterogeneous MOF glass imparted with unidirectional ion transport characteristic would be useful as an ion pump. This layered structure can potentially be constructed on a membrane substrate and applied in a reverse electrodialysis system for power generation. The main benefit of this heterogeneous MOF glass structure is that it blocks the back diffusion of ions, which can improve the energy conversion efficiency.[100] In addition, it can also potentially serve as a nanofluidic logic gate for logic computing devices.[120,121]

Moreover, it is envisioned that MOF glass can also be useful for electrochemical sensing applications. The abundance of under-coordinated or open metal sites in melt-quenched MOF glass is favourable not only for ion conduction, but can also serve as catalytic active sites for the oxidation or reduction of toxic inorganics such as heavy metals (Cd^{2+}, Cu^{2+}, Pb^{2+}, $Cr_2O_7^{2-}$).[53,122,123] It is clear that vast opportunities exist for the implementation of ionically conductive MOF glass beyond that as a solid state electrolyte due to the tunability of this material, which opens avenues for further research.

Conclusion

There has been a surge in interest over the recent years on a subgroup of amorphous MOF materials that undergoes a solid to liquid/glass phase transition, which are called MOF glasses. MOF glasses feature grain boundary-free and isotropic conduction pathways that can provide enhanced ion transport properties over the crystalline counterparts. This is particularly useful when they are applied as solid-state electrolytes, which tends to improve the stability and performance of batteries and fuel cells. Furthermore, they can be easily moulded into different shapes, and the high chemical reactivity of liquid MOF components upon heat treatment can promote contact and chemical interactions at an interface. This enables the interfacial engineering of ion transport properties in macroscopic devices. In order to aid the design of MOF glasses for ionic applications and direct future research efforts, we shed light on the underlying factors related to the pores, ligands and metal sites that govern ion conductivity and selectivity in these materials. It is envisioned that the high moldability and accessibility of meltable MOFs to the liquid state can be further exploited to create structures with unique ion transport properties, which offers exciting opportunities for the future development of these materials in this important area.

Conflicts of interest

There are no conflicts to declare.

Acknowledgements

We acknowledge financial support provided by the Australian Research Council DP180103874 and FT210100589. This research was supported by an AINSE Ltd Early Career Researcher Grant (ECRG).

References

1 S. R. Batten, N. R. Champness, X.-M. Chen, J. Garcia-Martinez, S. Kitagawa, L. Öhrström, M. O'Keeffe, M. P. Suh and J. Reedijk, *Pure Appl. Chem.*, 2013, **85**, 1715–1724.
2 L. Pilz, C. Natzeck, J. Wohlgemuth, N. Scheuermann, P. G. Weidler, I. Wagner, C. Wöll and M. Tsotsalas, *Adv. Mater. Interfaces*, 2023, **10**, 2201771.
3 M. Chai, S. Moradi, E. Erfani, M. Asadnia, V. Chen and A. Razmjou, *Chem. Mater.*, 2021, **33**, 8666–8676.
4 T. D. Bennett and A. K. Cheetham, *Acc. Chem. Res.*, 2014, **47**, 1555–1562.
5 H. Tuller, D. Button and D. R. Uhlmann, *J. Non-Cryst. Solids*, 1980, **40**, 93–118.
6 Y. Zheng, T. Qian, H. Ji, X. Xia, J. Liu, Y. Zhu and C. Yan, *Adv. Mater.*, 2021, **33**, 2102634.
7 L. Zhao, L. Zheng, X. Li, H. Wang, L.-P. Lv, S. Chen, W. Sun and Y. Wang, *ACS Appl. Mater. Interfaces*, 2021, **13**, 48913–48922.
8 P. J. Waller, F. Gándara and O. M. Yaghi, *Acc. Chem. Res.*, 2015, **48**, 3053–3063.
9 T. D. Bennett, Y. Yue, P. Li, A. Qiao, H. Tao, N. G. Greaves, T. Richards, G. I. Lampronti, S. A. Redfern, F. Blanc,

O. K. Farha, J. T. Hupp, A. K. Cheetham and D. A. Keen, *J. Am. Chem. Soc.*, 2016, **138**, 3484–3492.
10 H. Tao, T. D. Bennett and Y. Yue, *Adv. Mater.*, 2017, **29**, 1601705.
11 W. Chen, S. Horike, D. Umeyama, N. Ogiwara, T. Itakura, C. Tassel, Y. Goto, H. Kageyama and S. Kitagawa, *Angew. Chem., Int. Ed.*, 2016, **55**, 5195–5200.
12 T. Ogawa, K. Takahashi, S. S. Nagarkar, K. Ohara, Y. L. Hong, Y. Nishiyama and S. Horike, *Chem. Sci.*, 2020, **11**, 5175–5181.
13 N. Ma, S. Kosasang, A. Yoshida and S. Horike, *Chem. Sci.*, 2021, **12**, 5818–5824.
14 G. Jiang, C. Qu, F. Xu, E. Zhang, Q. Lu, X. Cai, S. Hausdorf, H. Wang and S. Kaskel, *Adv. Funct. Mater.*, 2021, **31**, 2104300.
15 J. Ren, C. Li, P. Li, S. Liu and L. Wang, *Chem. Eng. J.*, 2023, **462**, 142270.
16 C. Thanaphatkosol, N. Ma, K. Kageyama, T. Watcharatpong, T. Tiyawarakul, K. Kongpatpanich and S. Horike, *Chem. Commun.*, 2022, **58**, 6064–6067.
17 Y. Wang, H. Jin, Q. Ma, K. Mo, H. Mao, A. Feldhoff, X. Cao, Y. Li, F. Pan and Z. Jiang, *Angew Chem. Int. Ed. Engl.*, 2020, **59**, 4365–4369.
18 M. A. Ali, X. Liu, H.-T. Sun, J. Ren and J. Qiu, *Chem. Mater.*, 2022, **34**, 2476–2483.
19 J. A. Dawson, P. Canepa, T. Famprikis, C. Masquelier and M. S. Islam, *J. Am. Chem. Soc.*, 2018, **140**, 362–368.
20 H. Xia, H. Jin, Y. Zhang, H. Song, J. Hu, Y. Huang and Y. Li, *J. Membr. Sci.*, 2022, **655**, 120611.
21 V. Nozari, C. Calahoo, J. M. Tuffnell, P. Adelhelm, K. Wondraczek, S. E. Dutton, T. D. Bennett and L. Wondraczek, *Sci. Rep.*, 2020, **10**, 3532.
22 H. Lv, X. Zhao, H. Niu, S. He, Z. Tang, F. Wu and J. P. Giesy, *J. Hazard. Mater.*, 2019, **369**, 494–502.
23 A. F. Sapnik, D. N. Johnstone, S. M. Collins, G. Divitini, A. M. Bumstead, C. W. Ashling, P. A. Chater, D. S. Keeble, T. Johnson and D. A. Keen, *Dalton Trans.*, 2021, **50**, 5011–5022.
24 Y. Ohara, A. Hinokimoto, W. Chen, T. Kitao, Y. Nishiyama, Y.-l. Hong, S. Kitagawa and S. Horike, *Chem. Commun.*, 2018, **54**, 6859–6862.
25 S. Vaidya, O. Veselska, A. Zhadan, M. Diaz-Lopez, Y. Joly, P. Bordet, N. Guillou, C. Dujardin, G. Ledoux, F. Toche, R. Chiriac, A. Fateeva, S. Horike and A. Demessence, *Chem. Sci.*, 2020, **11**, 6815–6823.
26 P. Vervoorts, J. Keupp, A. Schneemann, C. L. Hobday, D. Daisenberger, R. A. Fischer, R. Schmid and G. Kieslich, *Angew. Chem.*, 2021, **133**, 800–806.
27 T. Ji, Y. Song, J. Yan, Y. Sun, C. Wang, S. Chen and Y. Liu, *Chem. Mater.*, 2022, **34**, 7878–7885.
28 L. N. McHugh and T. D. Bennett, *J. Mater. Chem. A*, 2022, **10**, 19552–19559.
29 L. Frentzel-Beyme, M. Kloss, P. Kolodzeiski, R. Pallach and S. Henke, *J. Am. Chem. Soc.*, 2019, **141**, 12362–12371.
30 M. Liu, R. D. McGillicuddy, H. Vuong, S. Tao, A. H. Slavney, M. I. Gonzalez, S. J. L. Billinge and J. A. Mason, *J. Am. Chem. Soc.*, 2021, **143**, 2801–2811.
31 V. Nozari, C. Calahoo, J. M. Tuffnell, D. A. Keen, T. D. Bennett and L. Wondraczek, *Nat. Commun.*, 2021, **12**, 5703.
32 V. Nozari, O. Smirnova, J. M. Tuffnell, A. Knebel, T. D. Bennett and L. Wondraczek, *Adv. Mater. Technol.*, 2022, **7**, 2200343.
33 Z. Yin, Y. Zhao, S. Wan, J. Yang, Z. Shi, S.-X. Peng, M.-Z. Chen, T.-Y. Xie, T.-W. Zeng, O. Yamamuro, M. Nirei, H. Akiba, Y.-B. Zhang, H.-B. Yu and M.-H. Zeng, *J. Am. Chem. Soc.*, 2022, **144**, 13021–13025.
34 Y. Zhao, S.-Y. Lee, N. Becknell, O. M. Yaghi and C. A. Angell, *J. Am. Chem. Soc.*, 2016, **138**, 10818–10821.
35 W. Xu, N. Hanikel, K. A. Lomachenko, C. Atzori, A. Lund, H. Lyu, Z. Zhou, C. A. Angell and O. M. Yaghi, *Angew. Chem., Int. Ed.*, 2023, e202300003.
36 M. A. Ali, W. M. W. Winters, M. A. Mohamed, D. Tan, G. Zheng, R. S. Madsen, O. V. Magdysyuk, M. Diaz-Lopez, B. Cai, N. Gong, Y. Xu, I. Hung, Z. Gan, S. Sen, H. Sun, T. D. Bennett, X. Liu, Y. Yue and J. Qiu, *Angew. Chem., Int. Ed. Engl.*, 2023, **62**, e202218094.
37 O. Basu, S. Mukhopadhyay, S. Laha and S. K. Das, *Chem. Mater.*, 2022, **34**, 6734–6743.
38 X. Wu, J. J. Hong, W. Shin, L. Ma, T. Liu, X. Bi, Y. Yuan, Y. Qi, T. W. Surta and W. Huang, *Nat. Energy*, 2019, **4**, 123–130.
39 X. Liang, F. Zhang, W. Feng, X. Zou, C. Zhao, H. Na, C. Liu, F. Sun and G. Zhu, *Chem. Sci.*, 2013, **4**, 983–992.
40 N. Agmon, *Chem. Phys. Lett.*, 1995, **244**, 456–462.
41 E. M. Miner, S. S. Park and M. Dincă, *J. Am. Chem. Soc.*, 2019, **141**, 4422–4427.
42 M. Farina, B. B. Duff, C. Tealdi, A. Pugliese, F. Blanc and E. Quartarone, *ACS Appl. Mater. Interfaces*, 2021, **13**, 53986–53995.
43 M. Inukai, Y. Nishiyama, K. Honjo, C. Das, S. Kitagawa and S. Horike, *Chem. Commun.*, 2019, **55**, 8528–8531.
44 O. Anderson and D. Stuart, *J. Am. Ceram. Soc.*, 1954, **37**, 573–580.
45 S. W. Martin, R. Christensen, G. Olson, J. Kieffer and W. Wang, *J. Phys. Chem. C*, 2019, **123**, 5853–5870.
46 R. Dutta and A. Kumar, *J. Mater. Sci.: Mater. Electron.*, 2019, **30**, 1117–1132.
47 D. K. McElfresh and D. G. Howitt, *J. Am. Ceram. Soc.*, 1986, **69**, 237–238.
48 P. Shirbhate, S. Vadrabade, S. Yawale and S. Pakade, *Ferroelectrics*, 2022, **587**, 70–75.
49 J. Hu, W. Wang, X. Zhu, S. Liu, Y. Wang, Y. Xu, S. Zhou, X. He and Z. Xue, *J. Membr. Sci.*, 2021, **618**, 118697.
50 N. Ma, N. Horike, L. Lombardo, S. Kosasang, K. Kageyama, C. Thanaphatkosol, K. Kongpatpanich, K.-i. Otake and S. Horike, *J. Am. Chem. Soc.*, 2022, **144**, 18619–18628.
51 J. M. Taylor, S. Dekura, R. Ikeda and H. Kitagawa, *Chem. Mater.*, 2015, **27**, 2286–2289.
52 B. M. Wiers, M.-L. Foo, N. P. Balsara and J. R. Long, *J. Am. Chem. Soc.*, 2011, **133**, 14522–14525.
53 R. Lin, X. Li, A. Krajnc, Z. Li, M. Li, W. Wang, L. Zhuang, S. Smart, Z. Zhu, D. Appadoo, J. R. Harmer, Z. Wang, A. G. Buzanich, S. Beyer, L. Wang, G. Mali, T. D. Bennett,

V. Chen and J. Hou, *Angew Chem. Int. Ed. Engl.*, 2022, **61**, e202112880.
54 H. Tang, X. Lv, J. Du, Y. Liu, J. Liu, L. Guo, X. Zheng, H. Hao and Z. Liu, *Appl. Organomet. Chem.*, 2022, **36**, e6777.
55 S. Fischer, J. Roeser, T. C. Lin, R. H. DeBlock, J. Lau, B. S. Dunn, F. Hoffmann, M. Fröba, A. Thomas and S. H. Tolbert, *Angew. Chem., Int. Ed.*, 2018, **57**, 16683–16687.
56 C. Zhou, L. Longley, A. Krajnc, G. J. Smales, A. Qiao, I. Erucar, C. M. Doherty, A. W. Thornton, A. J. Hill, C. W. Ashling, O. T. Qazvini, S. J. Lee, P. A. Chater, N. J. Terrill, A. J. Smith, Y. Yue, G. Mali, D. A. Keen, S. G. Telfer and T. D. Bennett, *Nat. Commun.*, 2018, **9**, 5042.
57 A. W. Thornton, K. E. Jelfs, K. Konstas, C. M. Doherty, A. J. Hill, A. K. Cheetham and T. D. Bennett, *Chem. Commun.*, 2016, **52**, 3750–3753.
58 L. Frentzel-Beyme, P. Kolodzeiski, J.-B. Weiß, A. Schneemann and S. Henke, *Nat. Commun.*, 2022, **13**, 7750.
59 Y. Feng, F.-C. Liang, Z.-Y. Huang, X.-X. Xie, S.-L. Cai, J. Fan, W.-G. Zhang and S.-R. Zheng, *Inorg. Chem.*, 2022, **61**, 16981–16985.
60 Z. Yang, Y. Belmabkhout, L. N. McHugh, D. Ao, Y. Sun, S. Li, Z. Qiao, T. D. Bennett, M. D. Guiver and C. Zhong, *Nat. Mater.*, 2023, **22**, 888–894.
61 S.-Q. Wang, X. Wang, X.-M. Cheng, J. Ma and W.-Y. Sun, *J. Mater. Chem. A*, 2022, **10**, 16396–16402.
62 A. M. Bumstead, I. Pakamorė, K. D. Richards, M. F. Thorne, S. S. Boyadjieva, C. Castillo-Blas, L. N. McHugh, A. F. Sapnik, D. S. Keeble, D. A. Keen, R. C. Evans, R. S. Forgan and T. D. Bennett, *Chem. Mater.*, 2022, **34**, 2187–2196.
63 J. Lu, H. Zhang, X. Hu, B. Qian, J. Hou, L. Han, Y. Zhu, C. Sun, L. Jiang and H. Wang, *ACS Nano*, 2020, **15**, 1240–1249.
64 Y. Guo, Y. Ying, Y. Mao, X. Peng and B. Chen, *Angew. Chem.*, 2016, **128**, 15344–15348.
65 R. N. Widmer, G. I. Lampronti, S. Anzellini, R. Gaillac, S. Farsang, C. Zhou, A. M. Belenguer, C. W. Wilson, H. Palmer, A. K. Kleppe, M. T. Wharmby, X. Yu, S. M. Cohen, S. G. Telfer, S. A. T. Redfern, F.-X. Coudert, S. G. MacLeod and T. D. Bennett, *Nat. Mater.*, 2019, **18**, 370–376.
66 A. M. Iskandarov and T. Tada, *Mater. Des.*, 2022, **222**, 111094.
67 T. Ogawa, K. Takahashi, T. Kurihara, S. S. Nagarkar, K. Ohara, Y. Nishiyama and S. Horike, *Chem. Mater.*, 2022, **34**, 5832–5841.
68 C. Orellana-Tavra, E. F. Baxter, T. Tian, T. D. Bennett, N. K. Slater, A. K. Cheetham and D. Fairen-Jimenez, *Chem. Commun.*, 2015, **51**, 13878–13881.
69 S. S. Nagarkar, S. Horike, T. Itakura, B. Le Ouay, A. Demessence, M. Tsujimoto and S. Kitagawa, *Angew. Chem., Int. Ed.*, 2017, **56**, 4976–4981.
70 Q. Dai, Z. Liu, L. Huang, C. Wang, Y. Zhao, Q. Fu, A. Zheng, H. Zhang and X. Li, *Nat. Commun.*, 2020, **11**, 13.
71 M. Abdollahzadeh, M. Chai, E. Hosseini, M. Zakertabrizi, M. Mohammad, H. Ahmadi, J. Hou, S. Lim, A. Habibnejad Korayem, V. Chen, M. Asadnia and A. Razmjou, *Adv. Mater.*, 2022, **34**, e2107878.
72 H. Xiao, M. Chai, M. Abdollahzadeh, H. Ahmadi, V. Chen, D. B. Gore, M. Asadnia and A. Razmjou, *Desalination*, 2022, **532**, 115733.
73 H. Xiao, M. Chai, A. Hosseini, A. H. Korayem, M. Abdollahzadeh, H. Ahmadi, V. Chen, D. B. Gore, M. Asadnia and A. Razmjou, *J. Membr. Sci.*, 2023, **670**, 121312.
74 J. Hou and H. Zhang, *Adv. Mater. Technol.*, 2023, **8**, 2201433.
75 X. Li, G. Jiang, M. Jian, C. Zhao, J. Hou, A. W. Thornton, X. Zhang, J. Z. Liu, B. D. Freeman and H. Wang, *Nat. Commun.*, 2023, **14**, 286.
76 J. Lu, H. Zhang, J. Hou, X. Li, X. Hu, Y. Hu, C. D. Easton, Q. Li, C. Sun and A. W. Thornton, *Nat. Mater.*, 2020, **19**, 767–774.
77 G. Eisenman and R. Horn, *J. Membr. Biol.*, 1983, **76**, 197–225.
78 D. Krauss, B. Eisenberg and D. Gillespie, *Eur. Biophys. J.*, 2011, **40**, 775–782.
79 M. Mohammad, M. Lisiecki, K. Liang, A. Razmjou and V. Chen, *Appl. Mater. Today*, 2020, **21**, 100884.
80 Y. Song, A. E. Khudozhitkov, J. Lee, H. Kang, D. I. Kolokolov, A. G. Stepanov and M. Yoon, *Chem. Commun.*, 2020, **56**, 4468–4471.
81 X. Miao, P. Wang, R. Sun, J. Li, Z. Wang, T. Zhang, R. Wang, Z. Li, Y. Bai, R. Hao and L. Yin, *Adv. Energy Mater.*, 2021, **11**, 2102396.
82 Z. Piao, H. R. Ren, G. Lu, K. Jia, J. Tan, X. Wu, Z. Zhuang, Z. Han, C. Li and R. Gao, *Angew. Chem., Int. Ed.*, 2023, **62**, e202300966.
83 C. Gao, Z. Jiang, S. Qi, P. Wang, L. R. Jensen, M. Johansen, C. K. Christensen, Y. Zhang, D. B. Ravnsbaek and Y. Yue, *Adv. Mater.*, 2022, **34**, e2110048.
84 L. Sun, H. Wang, S. Zhai, J. Sun, X. Fang, H. Yang, D. Zhai, C. Liu, W.-Q. Deng and H. Wu, *J. Energy Chem.*, 2023, **76**, 368–376.
85 J. Yan, C. Gao, S. Qi, Z. Jiang, L. R. Jensen, H. Zhan, Y. Zhang and Y. Yue, *Nano Energy*, 2022, **103**, 107779.
86 D. H. Tan, Y.-T. Chen, H. Yang, W. Bao, B. Sreenarayanan, J.-M. Doux, W. Li, B. Lu, S.-Y. Ham and B. Sayahpour, *Science*, 2021, **373**, 1494–1499.
87 E. Peled, *J. Electrochem. Soc.*, 1979, **126**, 2047.
88 Y.-X. Lin, Z. Liu, K. Leung, L.-Q. Chen, P. Lu and Y. Qi, *J. Power Sources*, 2016, **309**, 221–230.
89 J.-W. Park, S.-C. Jo, M.-J. Kim, I.-H. Choi, B. G. Kim, Y.-J. Lee, H.-Y. Choi, S. Kang, T. Kim and K.-J. Baeg, *NPG Asia Mater.*, 2021, **13**, 30.
90 F. Y. Fan, M. S. Pan, K. C. Lau, R. S. Assary, W. H. Woodford, L. A. Curtiss, W. C. Carter and Y.-M. Chiang, *J. Electrochem. Soc.*, 2016, **163**, A3111.
91 X. Zhang, G. Li, Y. Zhang, D. Luo, A. Yu, X. Wang and Z. Chen, *Nano Energy*, 2021, **86**, 106094.
92 R. K. Tonnah, M. Chai, M. Abdollahzadeh, H. Xiao, M. Mohammad, E. Hosseini, M. Zakertabrizi, D. Jarrahbashi, A. Asadi, A. Razmjou and M. Asadnia, *ACS Nano*, 2023, **17**, 12445–12457.

93 X. Li, H. Zhang, H. Yu, J. Xia, Y. B. Zhu, H. A. Wu, J. Hou, J. Lu, R. Ou and C. D. Easton, *Adv. Mater.*, 2020, **32**, 2001777.
94 J. Hou, P. Chen, A. Shukla, A. Krajnc, T. Wang, X. Li, R. Doasa, L. H. G. Tizei, B. Chan, D. N. Johnstone, R. Lin, T. U. Schülli, I. Martens, D. Appadoo, M. S. Ari, Z. Wang, T. Wei, S.-C. Lo, M. Lu, S. Li, E. B. Namdas, G. Mali, A. K. Cheetham, S. M. Collins, V. Chen, L. Wang and T. D. Bennett, *Science*, 2021, **374**, 621–625.
95 K. Ikigaki, K. Okada, Y. Tokudome, T. Toyao, P. Falcaro, C. J. Doonan and M. Takahashi, *Angew. Chem.*, 2019, **131**, 6960–6964.
96 L. Longley, S. M. Collins, C. Zhou, G. J. Smales, S. E. Norman, N. J. Brownbill, C. W. Ashling, P. A. Chater, R. Tovey, C.-B. Schönlieb, T. F. Headen, N. J. Terrill, Y. Yue, A. J. Smith, F. Blanc, D. A. Keen, P. A. Midgley and T. D. Bennett, *Nat. Commun.*, 2018, **9**, 2135.
97 L. Longley, S. M. Collins, S. Li, G. J. Smales, I. Erucar, A. Qiao, J. Hou, C. M. Doherty, A. W. Thornton, A. J. Hill, X. Yu, N. J. Terrill, A. J. Smith, S. M. Cohen, P. A. Midgley, D. A. Keen, S. G. Telfer and T. D. Bennett, *Chem. Sci.*, 2019, **10**, 3592–3601.
98 S. M. Collins, D. M. Kepaptsoglou, K. T. Butler, L. Longley, T. D. Bennett, Q. M. Ramasse and P. A. Midgley, *J. Am. Chem. Soc.*, 2018, **140**, 17862–17866.
99 S. M. Collins, K. E. MacArthur, L. Longley, R. Tovey, M. Benning, C.-B. Schönlieb, T. D. Bennett and P. A. Midgley, *APL Mater.*, 2019, **7**, 091111.
100 Z. Zhang, L. He, C. Zhu, Y. Qian, L. Wen and L. Jiang, *Nat. Commun.*, 2020, **11**, 875.
101 R. Li, J. Jiang, Q. Liu, Z. Xie and J. Zhai, *Nano Energy*, 2018, **53**, 643–649.
102 Z. Li, Y. Guo, X. Wang, P. Li, W. Ying, D. Chen, X. Ma, Z. Deng and X. Peng, *ACS Appl. Mater. Interfaces*, 2019, **11**, 34039–34045.
103 J. M. Tuffnell, C. W. Ashling, J. Hou, S. Li, L. Longley, M. L. R. Gomez and T. D. Bennett, *Chem. Commun.*, 2019, **55**, 8705–8715.
104 S. M. Haile, D. A. Boysen, C. R. Chisholm and R. B. Merle, *Nature*, 2001, **410**, 910–913.
105 N. Ma, S. Impeng, S. Bureekaew, N. Morozumi, M.-a. Haga and S. Horike, *J. Am. Chem. Soc.*, 2023, **145**, 9808–9814.
106 Z. Wang, K. Müller, M. Valášek, S. Grosjean, S. Bräse, C. Wöll, M. Mayor and L. Heinke, *J. Phys. Chem. C*, 2018, **122**, 19044–19050.
107 Y. Jiang, W. Ma, Y. Qiao, Y. Xue, J. Lu, J. Gao, N. Liu, F. Wu, P. Yu and L. Jiang, *Angew. Chem., Int. Ed.*, 2020, **59**, 12795–12799.
108 S. Tominaka and A. Cheetham, *RSC Adv.*, 2014, **4**, 54382–54387.
109 N. E. Wong, P. Ramaswamy, A. S. Lee, B. S. Gelfand, K. J. Bladek, J. M. Taylor, D. M. Spasyuk and G. K. Shimizu, *J. Am. Chem. Soc.*, 2017, **139**, 14676–14683.
110 R. Lin, J. Hou, M. Li, Z. Wang, L. Ge, S. Li, S. Smart, Z. Zhu, T. D. Bennett and V. Chen, *Chem. Commun.*, 2020, **56**, 3609–3612.
111 J. Hou, C. W. Ashling, S. M. Collins, A. Krajnc, C. Zhou, L. Longley, D. N. Johnstone, P. A. Chater, S. Li, M. V. Coulet, P. L. Llewellyn, F. X. Coudert, D. A. Keen, P. A. Midgley, G. Mali, V. Chen and T. D. Bennett, *Nat. Commun.*, 2019, **10**, 2580.
112 V. L. Martins, N. Sanchez-Ramirez, M. C. Ribeiro and R. M. Torresi, *Phys. Chem. Chem. Phys.*, 2015, **17**, 23041–23051.
113 C. Montoro, D. Rodríguez-San-Miguel, E. Polo, R. Escudero-Cid, M. L. Ruiz-González, J. A. Navarro, P. Ocón and F. Zamora, *J. Am. Chem. Soc.*, 2017, **139**, 10079–10086.
114 H. Chen, H. Tu, C. Hu, Y. Liu, D. Dong, Y. Sun, Y. Dai, S. Wang, H. Qian and Z. Lin, *J. Am. Chem. Soc.*, 2018, **140**, 896–899.
115 Z. Wang, R. Tan, H. Wang, L. Yang, J. Hu, H. Chen and F. Pan, *Adv. Mater.*, 2018, **30**, 1704436.
116 B. A. Paren, N. Nguyen, V. Ballance, D. T. Hallinan, J. G. Kennemur and K. I. Winey, *Macromolecules*, 2022, **55**, 4692–4702.
117 G. Guzmán-González, S. Vauthier, M. Alvarez-Tirado, S. Cotte, L. Castro, A. Guéguen, N. Casado and D. Mecerreyes, *Angew. Chem.*, 2022, **134**, e202114024.
118 S. M. Hossain, H. Yu, Y. Choo, G. Naidu, D. S. Han and H. K. Shon, *Desalination*, 2023, **546**, 116201.
119 Z. Li, C. Li, X. Liu, L. Cao, P. Li, R. Wei, X. Li, D. Guo, K.-W. Huang and Z. Lai, *Energy Environ. Sci.*, 2021, **14**, 3152–3159.
120 Y. Wang and J. Zhai, *Langmuir*, 2019, **35**, 3171–3175.
121 J. Li and D. Li, *J. Colloid Interface Sci.*, 2021, **596**, 54–63.
122 Z. Zhou, S. Mukherjee, S. Hou, W. Li, M. Elsner and R. A. Fischer, *Angew. Chem., Int. Ed.*, 2021, **60**, 20551–20557.
123 K. Zhu, R. Fan, J. Wu, B. Wang, H. Lu, X. Zheng, T. Sun, S. Gai, X. Zhou and Y. Yang, *ACS Appl. Mater. Interfaces*, 2020, **12**, 58239–58251.

